frontiers | Frontiers in Cellular and Infection Microbiology

TYPE Original Research
PUBLISHED 07 June 2024
DOI 10.3389/fcimb.2024.1411286

OPEN ACCESS

EDITED BY
Hani Harb,
Technical University Dresden, Germany

REVIEWED BY
Adam Valcek,
Vrije University Brussel, Belgium
Nadia Rodríguez-Medina,
National Institute of Public Health, Mexico

*CORRESPONDENCE
Katharina Schaufler
katharina.schaufler@helmholtz-hioh.de

†These authors have contributed equally to this work and share last authorship

RECEIVED 02 April 2024
ACCEPTED 23 May 2024
PUBLISHED 07 June 2024

CITATION
Müller JU, Schwabe M, Swiatek L-S, Heiden SE, Schlüter R, Sittner M, Bohnert JA, Becker K, Idelevich EA, Guenther S, Eger E and Schaufler K (2024) Temperatures above 37°C increase virulence of a convergent *Klebsiella pneumoniae* sequence type 307 strain. *Front. Cell. Infect. Microbiol.* 14:1411286. doi: 10.3389/fcimb.2024.1411286

Temperatures above 37°C increase virulence of a convergent *Klebsiella pneumoniae* sequence type 307 strain

Justus U. Müller[1], Michael Schwabe[1], Lena-Sophie Swiatek[1], Stefan E. Heiden[1], Rabea Schlüter[2], Max Sittner[1], Jürgen A. Bohnert[3], Karsten Becker[3], Evgeny A. Idelevich[3,4], Sebastian Guenther[5], Elias Eger[1†] and Katharina Schaufler[1,6*†]

[1]Department of Epidemiology and Ecology of Antimicrobial Resistance, Helmholtz Institute for One Health, Helmholtz Centre for Infection Research (HZI), Greifswald, Germany, [2]Imaging Center of the Department of Biology, University of Greifswald, Greifswald, Germany, [3]Friedrich Loeffler-Institute of Medical Microbiology, University Medicine Greifswald, Greifswald, Germany, [4]Institute of Medical Microbiology, University Hospital Münster, Münster, Germany, [5]Pharmaceutical Biology, Institute of Pharmacy, University of Greifswald, Greifswald, Germany, [6]University Medicine Greifswald, Greifswald, Germany

Background: Convergence of *Klebsiella pneumoniae* (KP) pathotypes has been increasingly reported in recent years. These pathogens combine features of both multidrug-resistant and hypervirulent KP. However, clinically used indicators for hypervirulent KP identification, such as hypermucoviscosity, appear to be differentially expressed in convergent KP, potential outbreak clones are difficult to identify. We aimed to fill such knowledge gaps by investigating the temperature dependence of hypermucoviscosity and virulence in a convergent KP strain isolated during a clonal outbreak and belonging to the high-risk sequence type (ST)307.

Methods: Hypermucoviscosity, biofilm formation, and mortality rates in *Galleria mellonella* larvae were examined at different temperatures (room temperature, 28°C, 37°C, 40°C and 42°C) and with various phenotypic experiments including electron microscopy. The underlying mechanisms of the phenotypic changes were explored via qPCR analysis to evaluate plasmid copy numbers, and transcriptomics.

Results: Our results show a temperature-dependent switch above 37°C towards a hypermucoviscous phenotype, consistent with increased biofilm formation and *in vivo* mortality, possibly reflecting a bacterial response to fever-like conditions. Furthermore, we observed an increase in plasmid copy number for a hybrid plasmid harboring carbapenemase and *rmpA* genes. However, transcriptomic analysis revealed no changes in *rmpA* expression at higher temperatures, suggesting alternative regulatory pathways.

Conclusion: This study not only elucidates the impact of elevated temperatures on hypermucoviscosity and virulence in convergent KP but also sheds light on previously unrecognized aspects of its adaptive behavior, underscoring its resilience to changing environments.

KEYWORDS

K. pneumoniae, temperature-dependent virulence, hypermucoviscosity, hypervirulence, plasmid copy number, transcriptomics

1 Introduction

The opportunistic pathogen *Klebsiella pneumoniae* is frequently associated with nosocomial infections worldwide including pneumonia, urinary tract, and bloodstream infections (Mathers et al., 2015). Classic, mostly nosocomial *K. pneumoniae* (cKp) often affects individuals with compromised immune systems (Lan et al., 2021) exacerbated by the rise of multidrug-resistant (MDR) representatives (Kochan et al., 2022).

Beyond the hospital walls, hypervirulent, *K. pneumoniae* (hvKp) strains can cause infections in healthy individuals (Choby et al., 2020). HvKp harbors a repertoire of key virulence factors such as siderophores (Russo and Marr, 2019). In recent years, the global emergence of converging pathotypes of *K. pneumoniae* strains contributed to difficult-to-treat infections, as they combine extensive drug resistance with hypervirulence mostly driven by hybrid plasmids (Shankar et al., 2022).

Traditionally, *K. pneumoniae* hypervirulence has been identified through a positive string test (Catalán-Nájera et al., 2017). This test explores "hypermucoviscosity", a characteristic associated with better evasion of macrophages contributing to the invasive potential of hvKp (Russo et al., 2018). Despite the assumption that hypervirulence and hypermucoviscosity are connected, there is evidence that hypermucoviscosity is not a peculiar marker of hypervirulence (Lee et al., 2006). Precise determination of hypervirulence involves *in vivo* experiments and specific genetic markers like *iucA* (hydroxamate siderophore), *iroB* (catecholate siderophore), and *rmpA* or *rmpA2* (regulator of the mucoid phenotype) (Russo et al., 2018). Hypermucoviscosity correlates with clinical outcomes such as pyogenic liver abscesses (Shon et al., 2013). While more than 79 serologically defined capsular types exist, and genomics continuously reveal further diversity in these surface antigens, they differ in composition, which impacts virulence and hypermucoviscosity (Follador et al., 2016; Lam et al., 2022). Especially monosaccharides such as mannose and rhamnose seem to play a role (Huang et al., 2022). Other complex biosynthetic and regulatory mechanisms responding to external stimuli such as iron availability and carbon sources are also involved (Mike et al., 2021). While mechanisms for bacterial adaptation to host temperatures are well-established, the impact of temperature changes within the host, such as fever episodes, on the regulation of virulence factors is not fully explored. Notably, there is a significant gap in understanding the temperature effects on hypermucoviscosity of *K. pneumoniae*, particularly above 37°C (Lam et al., 2014; Mandin and Johansson, 2020).

Here, we investigated capsule production and hypermucoviscosity in a convergent *K. pneumoniae* ST307 strain at different temperatures. By combining omics with *in vitro* and *in vivo* phenotypic experiments, we revealed temperature dependence of hypermucoviscosity and additional bacterial virulence, which are seemingly based on plasmid copy number (PCN)- and transcriptional changes.

2 Materials and methods

2.1 Bacterial strains (Table 1)

TABLE 1 Description of the investigated strain and its genetic properties, including Name, Species, Sequence type (capsule type), Plasmids and their main features.

Name	Species	ST (capsule type)	Plasmids and features
PBIO1953	*K. pneumoniae* (Heiden et al., 2020)	307 (KL102, O1/O2v2)	Plasmid 1 bla_{NDM-1}, *rmpA* Plasmid 2 $bla_{CTX-M-15}$ Plasmid 3 Plasmid 4 bla_{OXA-48} Plasmid 5

2.2 Hypermucoviscosity

In the string test, a sterile loop was applied to a single colony on an agar plate, which had been cultured at varying temperatures (28°C, 37°C, 40°C, 42°C) for a duration of 24 h. The loop was gently lifted, and if there was a 5 mm extension without breaking, the string test was considered positive, which characterizes hypermucoviscosity (Fang et al., 2004). Furthermore, the hypermucoviscosity was confirmed with the sedimentation assay as described previously (Mike et al., 2021). In short, 50 µL of a standardized bacterial suspension (0.5 McFarland standard turbidity in 0.9% (w/v) aqueous NaCl solution) was transferred

into 5 mL LB broth and was incubated at the desired temperature (RT, 28°C, 37°C, 40°C, 42°C) for 24 h. Afterwards, 1.5 mL of the 24 h culture was transferred into a 2 mL reaction tube and centrifuged for 1000 x g for 5 minutes, 200 µL from the supernatant as well as from the 24 h culture were pipetted as triplicates into a 96 well plate and the OD_{600} was measured with a plate reader (CLARIOstarplus, BMG Labtech, Ortenberg, Germany) (Eger et al., 2021).

The ability to generate exopolysaccharides was assessed using BHI agar plates supplemented with 5% sucrose (w/v) and 0.08% congo-red (w/v), following the methodology outlined in a prior study (Freeman et al., 1989). A single colony was picked up from an LB agar plate, streaked onto the stained BHI agar plates, and subsequently incubated overnight for 24 h at (RT, 28°C, 37°C, 38°C, 39°C, 40°C, 42°C). If the single colonies color black, they would be classified as positive for exopolysaccharides, while single colonies which are white to yellow would be considered negative for exopolysaccharide production.

2.3 Attachment and specific biofilm formation

The temperature influence on attachment factors was investigated with the crystal violet (CV) assay, as described previously (Schaufler et al., 2016; Eger et al., 2022) In short 50 µL of an overnight culture was transferred to 5 mL LB. After a visible turbidity samples were adjusted to an OD_{600} of 0.01 and 200 µL was transferred as into a 96 well plate. Afterwards, they were incubated at 28°C, 37°C, 40°C and 42°C for 24 h. Following the incubation, the OD_{600} was measured to determine the overall growth. Then, the supernatant of each well was discarded, the plate was washed three times with deionized water and dried for 10 min. Subsequently, fixed with 250 µL methanol for 15 min and then air dried for 15 min. Now the remaining cells were stained with 250 µL 1% crystal violet solution (w/v) for 30 min. This was followed by three washing steps with deionized water and drying for 10 min. The stained bacteria were dissolved with 300 µL of an ethanol acetone mixture with a ratio of 80 to 20 (v/v) and shaken for 30 min at 220 rpm at room temperature. Then the OD_{570} was measured. The specific biofilm formation (SBF) (Niu and Gilbert, 2004) was then calculated. The negative control was subtracted from the OD_{570} of the sample and then divided by the OD_{600} of the sample.

2.4 *Galleria mellonella in vivo* infection model

To test the influence of different temperatures on the pathogenic potential the *Galleria mellonella in vivo* infection model was used, as previously described (Insua et al., 2013) with slight adjustments of the experiment setup in respect to this temperature dependent study. Briefly, 2 mL of overnight culture of PBIO1953 was harvested and pelleted at 16000 x g for 5 min at RT. The pellet was once washed with PBS and diluted to an OD_{600} of 1.0. The 2×10^9 CFU/mL were further adjusted to 2×10^6 CFU/mL. The larvae (from Peter Zoopalast, Kiel, Germany) were randomly divided into 6 different groups of 10 individuals. 10 µL of the bacterial suspension was injected into the right proleg of the larvae. For the control groups 10 µL of PBS solution was used as injection, to check if the infection of *Galleria mellonella* larvae was affected by the traumata or the altered incubation temperature. The sample and control groups were incubated in a 90 mm glass petri dish at 28°C, 37°C and 40°C each. The vital state of the larvae was controlled every 24 h. The larvae were considered dead, if they showed strong pigmentation accompanied by not responding to physical stimuli. This assay was performed three independent times the results were pooled for each condition. a Kaplan-Meier plot was generated where the survival was plotted to visualize the mortality rates of the *Galleria mellonella* at different temperatures.

2.5 Plasmid copy number

To determine the plasmid copy numbers of the three largest plasmids (plasmid 1 bla_{NDM-1} and *rmpA*, plasmid 2 $bla_{CTX-M-15}$, plasmid 3) at different temperatures (RT, 28°C, 37°C, 40°C, 42°C) qPCR was used. Therefore, sets of different Primers seen in Supplementary Table 1 were designed to amplify a specific region on the gene constructs of interest. The primers were designed according to the manufacture's instruction for Luna qPCR Kit (New England Biolabs GmbH, Ipswich, MA, US) and ordered from Eurofins (Eurofins Genomics Europe Shared Services GmbH, Ebersberg, Germany).

The calibration for the plasmids (1–3) and the chromosome was performed with the Q5 High-Fidelity DNA Polymerase (New England Biolabs GmbH, Ipswich, MA, US) according to the manufacture's guideline, and isolated with NucleoSpin Gel and PCR Clean–up (MACHEREY-NAGEL GmbH & Co. KG, Düren, Germany) and quantified with the Qubit 4 fluorometer using the dsDNA HS Assay Kit (Thermo Fisher Scientific, Waltham, MA, USA). The qPCR was performed with the Luna qPCR protocol (New England Biolabs GmbH, Ipswich, MA, US) in regard to the qPCR cycler CFX Opus 96 Real-Time PCR System (Bio-Rad, Hercules, CA, US). Each sample was set up as seen in the Supplementary Table 2 and each sample was measured in triplicates following the protocol shown in Supplementary Table 3.

The measured concentration of the samples was related to the overall length of the gene structure and the plasmid copy number was calculated as

$$PCN = (P/C) * (Lc/Lp)$$

PCN: Plasmid copy number per genome equivalent P: Overall amount of the plasmid (in ng) C: Overall amount of the chromosome (in ng) Lc: Overall length of the chromosome (in base pairs) Lp: Overall length of the plasmid (in base pairs).

2.6 Electron microscopy

A single colony was inoculated into 30 mL of LB in an Erlenmeyer flask and cells were incubated at 28°C, 37°C, 40°C

and 42°C for 24 hours. Subsequently, the bacterial suspension was adjusted to OD_{600} = 1, and 1 mL of the suspension was diluted with 9 mL of 0.9% NaCl. The resulting suspension was then filtered through a hydrophilic polycarbonate filter (0.2 µm pore size, Merck Millipore). A segment of the filter was fixed with 1% glutaraldehyde and 4% paraformaldehyde in washing buffer (10 mM cacodylate buffer, 1 mM $CaCl_2$, 0.075% ruthenium red; pH 7) and then the samples were stored at 4°C until further processing (not more than 16 hours).

Samples were washed with washing buffer three times for 10 min each time, treated with 2% tannic acid in washing buffer for 1 h at RT, and then washed again with washing buffer three times for 15 minutes each time. Afterwards, the samples were dehydrated in a graded series of aqueous ethanol solutions (10, 30, 50, 70, 90, 100%) on ice for 15 min each step. Before the final change to 100% ethanol, samples were allowed to reach RT and then critical point-dried with liquid CO_2. Finally, the samples were mounted on aluminum stubs, sputtered with gold/palladium, and examined with a field emission scanning electron microscope Supra 40VP (Carl Zeiss Microscopy Deutschland GmbH, Oberkochen, Germany) using the Everhart-Thornley SE detector and the in-lens detector in a 70:30 ratio at an acceleration voltage of 5 kV. All micrographs were edited by using Adobe Photoshop CS6.

2.7 DNA isolation

The DNA isolation for the qPCR was performed by either 1 mL of 24 h cultures in LB at 28°C, 37°C, 40°C and 42°C or directly from the BHI agar plates supplemented with congo–red and sucrose incubated at the 4 different temperatures, where 4 to 6 single colonies were scraped off and resuspended via vortexing in 500 µL of PBS in a 1.5 mL test tube. The DNA isolation was then performed with the *MasterPure DNA Purification Kit for Blood* according to the manufacturer's specifications (Lucigen, Middleton, WI, USA). The quantification of the DNA was ensured by using the Qubit 4 fluorometer using the dsDNA HS Assay Kit (Thermo Fisher Scientific, Waltham, MA, USA).

2.8 RNA isolation and analyses

For transcriptomic analysis, the RNA was isolated from 50 mL liquid 24 h LB medium cultures (n=3) at 28°C, 37°C, 40°C and 42°C. 800 µL of the cultures were harvested in a 1.5 mL reaction tube and instantly chilled with liquid nitrogen for 5 s, to inhibit changes in the transcriptome. After the centrifugation (16,000 × *g* for 3 min at 2°C), the following RNA isolation was performed immediately with Monarch™ Total RNA Miniprep Kit (New England Biolabs GmbH, Ipswich, MA, US) according to the manufacture's instruction. The quality of the isolated RNA was tested using the Bioanalyzer with the Total RNA Nano Chip (Agilent, Santa Clara, CA, US). The samples were shipped on dry ice to Novogene (NOVOGENE COMPANY LTD., Cambridge, UK) for RNA sequencing (Illumina NovaSeq 6000; paired-end 150 bp).

The closed genome sequence of PBIO1953 was annotated with Bakta v. 1.7.0 and bakta database v. 5. In order to process the raw reads and to further quality trim the data, Trim Galore v. 0.6.8 (https://github.com/FelixKrueger/TrimGalore) was used. The trimmed reads were then mapped with Bowtie 2 v. 2.5.1 (mode: –very-sensitive-local), where the assembly of PBIO1953 was used as a reference. The gene counts were calculated using featureCounts v.2.0.1/stranded-mode) based on PBIO1953s´annotation. In the following step, the count table was imported into R v. 4.3.1 (https://www.R-project.org/), and differentially expressed genes were identified with DESeq2 v. 1.40.0 in default mode, with one exception; genes with rowSums of <10 in the count table were excluded before the analysis. Within our analyses, we used an absolute log2 fold change 1.5 thresholds combined with an adjusted e value lower than 0.05 to determine differences within gene expression, between the different incubation conditions. We excluded one replicate which was incubated at 37°C due to a shift on principal component 1 (PC1) and PC2, which can be seen in Supplementary Figure S2 where principal-component analysis is plotted. Finally, all genes were annotated using the online tool eggnog-mapper v. 2.1.9 to extract COG (cluster of orthologous groups) categories.

2.9 Statistical analysis

Statistical analyses were conducted using GraphPad Prism v. 9.5.1 for Windows, developed by GraphPad Software (San Diego, CA US). To assess qPCR results, the Bio-Rad CFX Maestro 2.3 v. 5.3.0 22.1030 (Bio-Rad, Hercules, CA, US) was utilized. All phenotypic experiments consisted of three or more independent biological replicates. Unless otherwise specified, data were presented as the mean and standard deviation. Statistical significance was determined using *p* values below 0.05 to indicate significant differences among the results.

2.10 Ethic statement

Ethical approval for this study was obtained from the ethics committee of the University of Greifswald, Germany (Approval number: BB 133/20), ensuring compliance with established ethical standards. Informed consent from patients was waived as samples were collected under a hospital surveillance framework for routine sampling. The study strictly adheres to the principles outlined in the Helsinki Declaration. No identifiable patient data, such as names and ages, was included in the study, and no tissue samples were utilized during isolation procedures.

3 Results

We investigated hypermucoviscosity and mortality for a previously published, convergent *K. pneumoniae* ST307 strain [PBIO1953 as described in Table 1 (Heiden et al., 2020)] at RT, 28°C, 37°C, 40°C, and 42°C (Figure 1). First, we stained capsular exopolysaccharides (Figure 1A). Here, white to yellow-beige colonies indicate "normal" exopolysaccharide production, which

10.3389/fcimb.2024.1411286

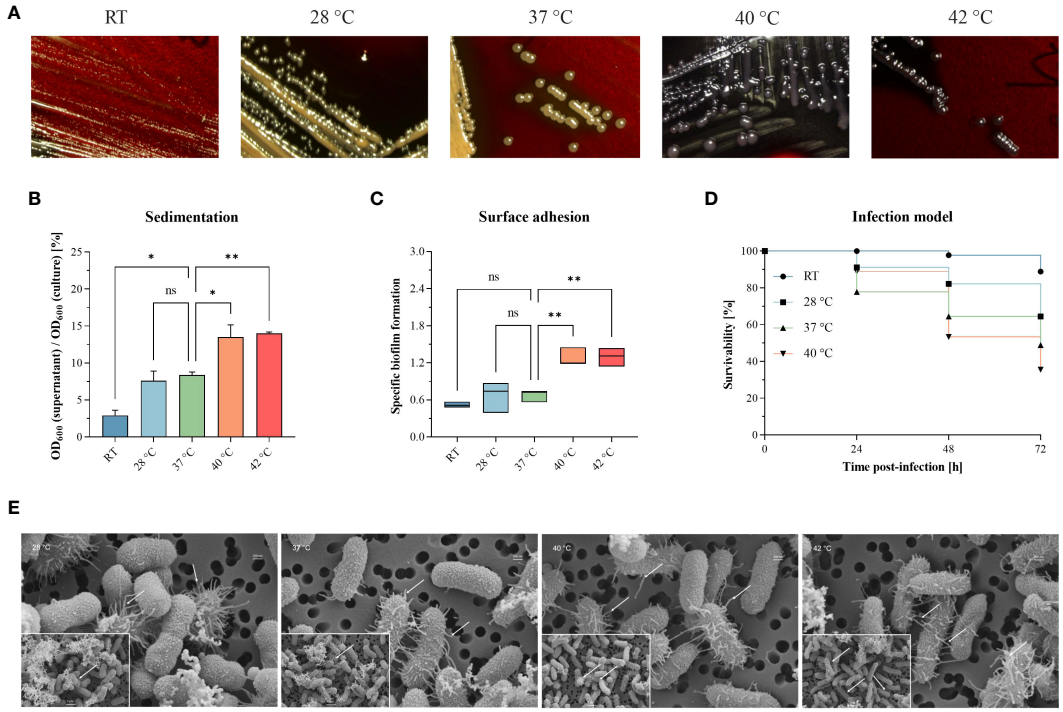

FIGURE 1
Different temperatures affect mucoviscosity and overall virulence of the convergent *K pneumoniae* ST307 strain PBIO1953. **(A)** Staining of capsular polysaccharides revealed a temperature-dependent change from a "normal" mucoid phenotype (yellow-beige colonies) to a hypermucoid phenotype (black colonies) at 40°C and 42°C. **(B)** The hypermucoviscosity was associated with a decrease in sedimentation upon centrifugation at 1,000 x g for 5 min. Results are shown as mean and standard error of percentage OD_{600} remaining in the supernatant after centrifugation (n = 3). **(C)** Temperatures above 37°C resulted in increased adhesion to plastic surfaces. Results are expressed as growth-adjusted specific biofilm formation. The line in the box indicates the median value (n = 3). **(D)** The *in vivo* infection model showed a temperature-dependent increase in mortality rates. Kaplan-Meier plot of survivability rates of the *G. mellonella* larvae (n = 30). Results are expressed as mean percent of survivability after injection of 10^5 CFU/larvae. For all results, mucoviscosity-associated characteristics at the different temperatures were compared to 37°C using analysis of variance (one-way ANOVA with Dunnett's multiple comparison *post hoc* test); ns, not significant; P* <0.05; **P <0.01. RT, room temperature. **(E)** Scanning electron micrographs of PBIO1953 at 28°C, 37°C, 40°C, and 42°C at 20,000x magnification, scale bar = 200 nm (inserts: 10,000x magnification, scale bar = 1 µm), arrowheads show fimbriae-like structures.

applied to PBIO1953 at RT, 28°C, and 37°C. In contrast, black colonies appeared above 37°C (Figure 1A; Supplementary Figure S6), implying increased polysaccharide biosynthesis (Freeman et al., 1989). String tests confirmed these result (data not shown), hypermucoviscosity was identified at 40°C and 42°C. The sedimentation assay also confirmed higher viscosity at 40°C (p = 0.0325) and 42°C (p = 0.0187) compared to 37°C, indicating hypermucoviscosity (Figure 1B). During our examination of a control for hvKp and a non-mucoid strain, we found no evidence of temperature dependence in contrast to PBIO1953, as illustrated in Supplementary Figure S7. Third, biofilm experiments revealed that increasing temperatures led to higher affinity of PBIO1953 to adhere to abiotic surfaces (Figure 1C). A significant increase in specific biofilm formation was observed at 40°C (p = 0.0053) and 42°C (p = 0.0049) in comparison to 37°C. Interestingly, this was not related to curli or cellobiose production (Supplementary Figure S1).

Finally, to explore the impact of different temperatures on the overall virulence of PBIO1953, we assessed mortality rates in *Galleria (G.) mellonella* larvae (Figure 1D). After 24 hours, mortality rates at 37°C (22.22%) exceeded those observed at 40°C (11.12%). However, 48 hours post-infection, mortality rates at 40°C consistently exceeded those at 37°C, with a peak after 72 hours. As control, the larvae were mock-infected with PBS and incubated at RT, 28°C, 37°C, 40°C with no detected temperature influence on the larvae mortality (Supplementary Figure S3). At all temperatures tested, the death of the larvae was always accompanied by a dark brown to blackish coloration of the carcass, which indicates the activity of the larvae's immune system before death (Pereira et al., 2020). Furthermore, there were no signs of an active immune system in the mock-infected larvae incubated at different temperatures (RT, 28°C, 37°C, 40°C). Note that incubation of mock-infected *G. mellonella* larvae at 42°C resulted in mortality rates greater than 10% [data not shown e.g (Ménard et al., 2021)].

Interestingly, scanning electron micrographs indicate an increasing amount of virulence- and biofilm-associated fimbriae structures at elevated temperatures of 40°C and 42°C compared to lower temperatures of 28°C and 37°C (Figure 1E). The fimbriae-like structures appear as thin, filamentous appendages extending from the bacterial surface. These structures exhibit a thread-like morphology, characterized by their elongated and slender appearance. They are typically distributed across the bacterial surface, appearing as protrusions or projections that emanate from the cell wall. The presence of these structures is marked by the placement of small white arrows in the micrographs, indicating their location and

abundance. While individual fimbriae may vary in length and thickness, their collective presence forms a distinctive pattern across the bacterial surface. It is important to note that the bacterial capsule appears compromised during the staining process. Nevertheless, the visible increase of these structures at higher temperatures (40°C, 42°C) implies a temperature-associated regulation (Chen et al., 2011).

3.1 Different temperatures affect PCN

To explore the underlying mechanisms, PCN-variations were measured using qPCR. Previously, we have shown that the convergent PBIO1953 strain harbors five different plasmids, one of which is a hybrid plasmid (plasmid 1) encoding both AMR and hypervirulence genes (Heiden et al., 2020). The three largest PBIO1953 plasmids were included in the subsequent analysis: plasmid 1 (360,596 bp), positive for the metallo-β-lactamase gene $bla_{\text{NDM-1}}$ and the regulator of the mucoid phenotype *rmpA*, plasmid 2 (130,131 bp) encoding the extended-spectrum β-lactamase (ESBL) gene $bla_{\text{CTX-M-15}}$, and plasmid 3 (72,679 bp) without any resistance genes (Figure 2).

As the hypermucoviscosity switch was observed above 37°C, we normalized all PCN to 37°C. Interestingly, the PCN differed not only based on the different temperatures but also regarding the respective plasmid and experimental set-ups (Figure 2). For the hybrid plasmid 1, the PCN increased with higher temperatures, with the highest value obtained at 42°C. The PCN of plasmid 2 did not show a clear temperature decency, but a PCN reduction was apparent at both 28°C and 42°C in the liquid culture set-up. Plasmid 3 showed a PCN decreasing with higher temperatures.

3.2 Temperature-dependent transcriptomic changes

For transcriptomics, we first focused on genes displaying differential gene expression (DGE) at 28°C, 40°C and 42°C (e-value < 0.05, |log2fold| change > 1.5) in comparison to 37°C. DGE appeared mostly between 28°C and 37°C (Supplementary Figures S4, S5), while, at 37°C compared to 40°C and 42°C, we only noticed few differentially expressed genes. Our initial hypothesis that *rmpA* would be differentially expressed was rejected and, genes related to the capsular gene cluster were unaffected.

When comparing 28°C-associated gene expression to 37°C (and 40°C and 42°C), we observed various, significant changes. Notably, the chromosomally located *ibpAB* gene and two small heat shock proteins encoded on plasmid 2, exhibited differential expression at increased temperatures. These genes are known for mitigating growth defects under thermal stress (Kitagawa et al., 2000). Furthermore, we observed the upregulation of several stress-related genes at 37°C and higher, including the Fur repressor, which possesses protective properties against reactive oxygen species (Achenbach and Yang, 1997) and *sodA*, a gene involved in radical scavenging. Of particular interest was the upregulation of *acrAB*, known for its role in antimicrobial resistance and virulence (Padilla et al., 2010). Remarkably, the expression of *mrkABCD*, which encodes the type 3 fimbriae system, increased at 37°C and above. Previous research has suggested that environmental factors (Johnson et al., 2011), like temperature, can impact attachment factors, making this observation particularly intriguing. Conversely, we noted a downregulation of *fimHGFDCIA*, responsible for the expression of fimbriae type 1 (Struve et al., 2008), and the downregulation of the *rfb* gene, which encodes O-antigens (Kelly and Whitfield, 1996). Additionally, *ompA*, a known virulence factor and key element in immune system recognition (Llobet et al., 2009) was downregulated at increased temperatures. On plasmid 1, the partitioning system *parAB* responsible for segregation and plasmid stability (Bignell and Thomas, 2001) demonstrated increased expression at higher temperatures. Notably, genes associated with transposon activation and IS sequences were also upregulated on plasmid 1. The gene *iutA*, encoding aerobactin and contributing to bacterial virulence, was upregulated at 37°C (and 40°C and 42°C). Moreover, on plasmid 2, the metallo-resistance gene *arsR* was upregulated (Xu et al., 1996). Finally, plasmids 4 and 5 showed increased expression of genes involved in conjugative transfer, including *traA* (Yang et al., 2007) and *mobC* (Zhang and Meyer, 1997). When comparing the transcriptomes of 40°C to those at 37°C, DGE was observed in six genes. Notably, two downregulated genes, *metR* (associated with the methionine pathway) and *argC* (linked to the arginine pathway), were particularly interesting as they are important for general growth. Only two genes were

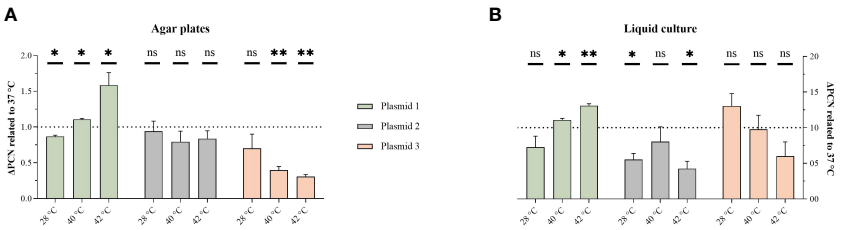

FIGURE 2
Temperature variation affect PCN. The PCN was determined from individual colonies grown on congo-red-dye-enriched agar plates **(A)** or from cells pelleted from sedimentation assay cultures **(B)**. The results are expressed as mean and standard error (one sample t-test in comparison to 1 at 37°C ns, not significant P* <0.05; P** <0.01, P** < 0.001.).

upregulated, with *betB* standing out as this gene is involved in the biosynthesis of osmoprotective choline-glycine betadine (Landfald and Str0m, 1986). Similarly, the comparison of 42°C to 37°C revealed six differentially expressed genes. *BetB* demonstrated concordance with the upregulated genes at 40°C. An intriguing finding was the upregulation of *pecM*, a gene previously implicated as a potential deactivator of the *fim* operon and a member of the permease of the drug/metabolite transporter (DMT) superfamily.

4 Discussion

Hypermucoviscosity is often referred to as the most important virulence characteristic of hvKp. However, it is largely unclear how external stressors can affect capsule expression and thus virulence in bacteria, especially in convergent *K. pneumoniae*. We revealed that a convergent *K. pneumoniae* ST307 outbreak strain (Heiden et al., 2020), changed from a "normal" to a hypermucoid and pronounced virulent phenotype upon temperature exposure above the healthy human body temperature at about 37°C.

Bacterial capsule formation is a highly complex process influenced by several internal and external factors. Although hvKp frequently exhibits capsule types K1 and K2, a clear correlation between the capsule type and hypervirulence has not yet been established (Pan et al., 2008). To our knowledge, we are the first to report a temperature-dependent phenotypic switch for *K. pneumoniae*. Previously, Le et al. (2022) have shown that temperatures below 37°C may affect hypermucoviscosity, based on the presence of plasmid-encoded *rmpA* at 37°C when compared to RT (Le et al., 2022). In contrast, our results suggest that *rmpA*, although plasmid-encoded, was not differentially expressed at different temperatures. More importantly, the increased PCN plasmid 1 does seemingly not have any effect on *rmpA* expression, although it is known that higher gene abundance as a result of increased PCN can lead to higher gene expression. It seems likely that hypermucoviscosity does not exclusively depend on *rmpA* expression. This assumption has been previously supported by studies where *K. pneumoniae* isolates harbor impaired capsule locus genes and the respective regulator but show hypermucoviscosity (Dey et al., 2022)

While a substantial number of genes exhibited DGE between 28°C and 37°C, only a limited number of genes was differentially regulated at 37°C vs. 40°C or 42°C. For all comparisons, most of the differentially expressed genes were chromosomally encoded, which suggests that increasing temperatures up to pathophysiological conditions (i.e., fever) does not lead to major shifts in the transcriptome and to the phenotypic switch. Rather, this seems to fine-tune the expression of a small number of genes together with the different PCN. We surmise that temperature-dependent stress regulators and heat shock proteins may be involved in the regulation of capsule production, which is supported by previous studies (Dorman et al., 2018). However, why the upregulation of stress response regulators and proteins, which normally control the expression of a large number of protein-associated genes (Kitagawa et al., 2000), does not lead to a clearer change in the bacterial transcriptome, remains unclear. The only direct regulatory pathway previously connected to capsule synthesis and influenced by increased temperatures was the *rcsA* gene, which contributes to capsular overexpression and is usually expressed at temperatures below 37°C (McCallum and Whitfield, 1991). Note that this is contrary to our findings.

Here, we identified a link between hypermucoviscosity and fimbrial regulation. The upregulation of type 3 fimbriae at temperatures above 28°C might be responsible for the fimbrial-like structures at higher temperatures as visualized by scanning electron microscopy. Interestingly, Lin et al. (2011) showed that hypermucoviscosity and type 3 fimbriae production can be co-regulated and depend on iron availability, and that iron limitation results in a reduction of mucoviscosity and fimbriae expression (Lin et al., 2011). Conversely, we observed a downregulation of type 1 fimbriae at higher temperatures. This might be because type 1 and type 3 fimbriae are independently regulated. However, in the CV assay, which measures specific biofilm formation, increased attachment at 40°C (and 42°C) compared to 37°C was measured, indicating a higher cell-to-cell and cell-to-plastic adherence, which could be fimbriae type 3-related and is essential in the transition from a planktonic to a multicellular lifestyle.

We speculate that PBIO1953 has evolved specific mechanisms to respond to the host's immune system, combined with a temperature-dependent formation of a physical capsule barrier and increased attachment at 40°C and 42°C. In the *in vivo* infection model, higher mortality was initially achieved after 24 hours at 37°C than at 40°C, which may be due to the initial encapsulation process combined with higher adherence at 40°C. As a result, the immune system response may be impeded, enabling bacterial proliferation. After 48 h and 72 h, we noticed a subsequent mortality increase at 40°C, again hinting towards better bacterial proliferation, possibly due to encapsulation and the previously mentioned changes. Similar has been previously suggested for various pathogens (Finlay and McFadden, 2006) but not *Klebsiella*. At the same time, we must acknowledge that our results are based on RNA sequencing data with stringent cut-offs and obtained from 24 h liquid cultures, which adds uncertainty when trying to apply these findings to *in vivo* situations. However, the general influence of the temperature on the *Klebsiella* strain could be observed and thus make general assumption on the *in vivo* situation possible. A further limitation is the fact that we only investigated a single *K. pneumoniae* strain. Prospective studies will have to explore whether similar applies to other strains. Nevertheless, our results suggest that enhanced temperatures and thus pathological conditions (i.e., fever) can lead to increased bacterial virulence, further exacerbating the overall tense situation. However, hypermucoviscosity could also represent a vulnerability that could be considered in a future treatment strategy.

We show that increased temperatures and thus potentially pathological conditions led to increased virulence in a convergent *K. pneumoniae* strain, which might play a pivotal role in shaping the dynamics of infection processes. In addition, our study contributes to a better understanding of the underlying mechanisms leading to hypermucoviscosity and *in vivo* bacterial virulence.

Data availability statement

The transcriptomic data for this study have been deposited in the European Nucleotide Archive (ENA) at EMBL-EBI under accession number PRJEB72193 (https://www.ebi.ac.uk/ena/browser/view/PRJEB72193). Additional genomic data of PBIO1953 are available under accession number PRJEB37933 (https://www.ebi.ac.uk/ena/browser/view/PRJEB37933).

Ethics statement

The studies involving humans were approved by ethics committee of the University of Greifswald, Germany (Approval number: BB 133/20). The studies were conducted in accordance with the local legislation and institutional requirements. The ethics committee/institutional review board waived the requirement of written informed consent for participation from the participants or the participants' legal guardians/next of kin because Ethical approval for this study was obtained from the ethics committee of the University of Greifswald, Germany (Approval number: BB 133/20), ensuring compliance with established ethical standards. Informed consent from patients was waived as samples were collected under a hospital surveillance framework for routine sampling. The study strictly adheres to the principles outlined in the Helsinki Declaration. No identifiable patient data, such as names and ages, was included in the study, and no tissue samples were utilized during isolation procedures. The manuscript presents research on animals that do not require ethical approval for their study.

Author contributions

JM: Data curation, Formal analysis, Investigation, Methodology, Visualization, Writing – original draft. MiS: Data curation, Formal analysis, Software, Writing – review & editing. LS: Formal analysis, Methodology, Writing – review & editing. SH: Data curation, Formal analysis, Software, Writing – review & editing. RS: Formal analysis, Investigation, Methodology, Writing – review & editing. MaS: Formal analysis, Writing – review & editing. JB: Formal analysis, Writing – review & editing. KB: Formal analysis, Writing – review & editing. EI: Formal analysis, Writing – review & editing. SG: Formal analysis, Writing – review & editing. EE: Writing – review & editing, Formal analysis, Investigation, Methodology, Validation, Writing – original draft. KS: Conceptualization, Data curation, Funding acquisition, Project administration, Resources, Supervision, Validation, Writing – review & editing.

Funding

The author(s) declare financial support was received for the research, authorship, and/or publication of this article. This work and the positions of LS, JM and MS were supported by a grant from the Federal Ministry of Education and Research (BMBF) to KS entitled "Disarming pathogens as a different strategy to fight antimicrobial-resistant Gram-negatives" Federal Ministry of Education and Research [grant no 01KI2015].

Acknowledgments

We thank Sara-Lucia Wawrzyniak for her excellent technical assistance as well as Stefan Bock for excellent technical assistance regarding electron microscopy.

Conflict of interest

The authors declare that the research was conducted in the absence of any commercial or financial relationships that could be construed as a potential conflict of interest.

The author(s) declared that they were an editorial board member of Frontiers, at the time of submission. This had no impact on the peer review process and the final decision.

Publisher's note

Supplementary material

The Supplementary Material for this article can be found online at: https://www.frontiersin.org/articles/10.3389/fcimb.2024.1411286/full#supplementary-material

References

Achenbach, L. A., and Yang, W. (1997). The fur gene from Klebsiella pneumoniae: characterization, genomic organization and phylogenetic analysis. *Gene* 185, 201–207. doi: 10.1016/S0378-1119(96)00642-7

Bignell, C., and Thomas, C. M. (2001). The bacterial ParA-ParB partitioning proteins. *J. Biotechnol.* 91, 1–34. doi: 10.1016/S0168-1656(01)00293-0

Catalán-Nájera, J. C., Garza-Ramos, U., and Barrios-Camacho, H. (2017). Hypervirulence and hypermucoviscosity: Two different but complementary Klebsiella spp. phenotypes? *Virulence* 8, 1111–1123. doi: 10.1080/21505594.2017.1317412

Chen, F.-J., Chan, C.-H., Huang, Y.-J., Liu, K.-L., Peng, H.-L., Chang, H.-Y., et al. (2011). Structural and mechanical properties of Klebsiella pneumoniae type 3 Fimbriae. *J. Bacteriol.* 193, 1718–1725. doi: 10.1128/JB.01395-10

Choby, J. E., Howard-Anderson, J., and Weiss, D. S. (2020). Hypervirulent Klebsiella pneumoniae - clinical and molecular perspectives. *J. Internal Med.* 287, 283–300. doi: 10.1111/joim.13007

Dey, T., Chakrabortty, A., Kapoor, A., Warrier, A., Nag, V. L., Sivashanmugam, K., et al. (2022). Unusual hypermucoviscous clinical isolate of klebsiella pneumoniae with

no known determinants of hypermucoviscosity. *Microbiol. Spectr.* 10, e0039322. doi: 10.1128/spectrum.00393-22

Dorman, M. J., Feltwell, T., Goulding, D. A., Parkhill, J., and Short, F. L. (2018). The capsule regulatory network of klebsiella pneumoniae defined by density-traDISort. *MBio* 9. doi: 10.1128/mBio.01863-18

Eger, E., Domke, M., Heiden, S. E., Paditz, M., Balau, V., Huxdorff, C., et al. (2022). Highly virulent and multidrug-resistant escherichia coli sequence type 58 from a sausage in Germany. *Antibio. (Basel Switzerland)* 11. doi: 10.3390/antibiotics11081006

Eger, E., Heiden, S. E., Becker, K., Rau, A., Geisenhainer, K., Idelevich, E. A., et al. (2021). Hypervirulent klebsiella pneumoniae sequence type 420 with a chromosomally inserted virulence plasmid. *Int. J. Mol. Sci.* 22. doi: 10.3390/ijms22179196

Fang, C.-T., Chuang, Y.-P., Shun, C.-T., Chang, S.-C., and Wang, J.-T. (2004). A novel virulence gene in Klebsiella pneumoniae strains causing primary liver abscess and septic metastatic complications. *J. Exp. Med.* 199, 697–705. doi: 10.1084/jem.20030857

Finlay, B. B., and McFadden, G. (2006). Anti-immunology: Evasion of the host immune system by bacterial and viral pathogens. *Cell* 124, 767–782. doi: 10.1016/j.cell.2006.01.034

Follador, R., Heinz, E., Wyres, K. L., Ellington, M. J., Kowarik, M., Holt, K. E., et al. (2016). The diversity of Klebsiella pneumoniae surface polysaccharides. *Microbial Genomics* 2. doi: 10.1099/mgen.0.000073

Freeman, D. J., Falkiner, F. R., and Keane, C. T. (1989). New method for detecting slime production by coagulase negative staphylococci. *J. Clin. Pathol.* 42, 872–874. doi: 10.1136/jcp.42.8.872

Heiden, S. E., Hübner, N.-O., Bohnert, J. A., Heidecke, C.-D., Kramer, A., Balau, V., et al. (2020). A Klebsiella pneumoniae ST307 outbreak clone from Germany demonstrates features of extensive drug resistance, hypermucoviscosity, and enhanced iron acquisition. *Genome Med.* 12, 113. doi: 10.1186/s13073-020-00814-6

Huang, X., Li, X., An, H., Wang, J., Ding, M., Wang, L., et al. (2022). Capsule type defines the capability of Klebsiella pneumoniae in evading Kupffer cell capture in the liver. *PloS Pathog.* 18. doi: 10.1371/journal.ppat.1010693

Insua, J. L., Llobet, E., Moranta, D., Pérez-Gutiérrez, C., Tomás, A., Garmendia, J., et al. (2013). Modeling Klebsiella pneumoniae pathogenesis by infection of the wax moth Galleria mellonella. *Infect. Immun.* 81, 3552–3565. doi: 10.1128/IAI.00391-13

Johnson, J. G., Murphy, C. N., Sippy, J., Johnson, T. J., and Clegg, S. (2011). Type 3 fimbriae and biofilm formation are regulated by the transcriptional regulators MrkHI in Klebsiella pneumoniae. *J. Bacteriol.* 193, 3453–3460. doi: 10.1128/JB.00286-11

Kelly, R. F., and Whitfield, C. (1996). Clonally diverse rfb gene clusters are involved in expression of a family of related D-galactan O antigens in Klebsiella species. *J. Bacteriol.* 178, 5205–5214. doi: 10.1128/jb.178.17.5205-5214.1996

Kitagawa, M., Matsumura, Y., and Tsuchido, T. (2000). Small heat shock proteins, IbpA and IbpB, are involved in resistances to heat and superoxide stresses in Escherichia coli. *FEMS Microbiol. Lett.* 184, 165–171. doi: 10.1111/fml.2000.184.issue-2

Kochan, T. J., Nozick, S. H., Medernach, R. L., Cheung, B. H., Gatesy, S. W. M., Lebrun-Corbin, M., et al. (2022). Genomic surveillance for multidrug-resistant or hypervirulent Klebsiella pneumoniae among United States bloodstream isolates. *BMC Infect. Dis.* 22, 603. doi: 10.1186/s12879-022-07558-1

Lam, M. M. C., Wick, R. R., Judd, L. M., Holt, K. E., and Wyres, K. L. (2022). Kaptive 2.0: updated capsule and lipopolysaccharide locus typing for the Klebsiella pneumoniae species complex. *Microbial Genomics* 8. doi: 10.1099/mgen.0.000800

Lam, O., Wheeler, J., and Tang, C. M. (2014). Thermal control of virulence factors in bacteria: A hot topic. *Virulence* 5, 852–862. doi: 10.4161/21505594.2014.970949

Lan, P., Jiang, Y., Zhou, J., and Yu, Y. (2021). A global perspective on the convergence of hypervirulence and carbapenem resistance in Klebsiella pneumoniae. *J. Global Antimicrobial Res.* 25, 26–34. doi: 10.1016/j.jgar.2021.02.020

Landfald, B., and Str0m, A. R. (1986). Choline-glycine betaine pathway confers a high level of osmotic tolerance in escherichia coli. *J. Bacteriol.* 165 (3), 849–855. doi: 10.1128/jb.165.3.849-855.1986

Le, M. N.-T., Kayama, S., Wyres, K. L., Yu, L., Hisatsune, J., Suzuki, M., et al. (2022). Genomic epidemiology and temperature dependency of hypermucoviscous Klebsiella pneumoniae in Japan. *Microbial Genomics* 8. doi: 10.1099/mgen.0.000827

Lee, H.-C., Chuang, Y.-C., Yu, W.-L., Lee, N.-Y., Chang, C.-M., Ko, N.-Y., et al. (2006). Clinical implications of hypermucoviscosity phenotype in Klebsiella pneumoniae isolates: association with invasive syndrome in patients with community-acquired bacteraemia. *J. Internal Med.* 259, 606–614. doi: 10.1111/j.1365-2796.2006.01641.x

Lin, C.-T., Wu, C.-C., Chen, Y.-S., Lai, Y.-C., Chi, C., Lin, J.-C., et al. (2011). Fur regulation of the capsular polysaccharide biosynthesis and iron-acquisition systems in Klebsiella pneumoniae CG43. *Microbiol. (Reading England)* 157, 419–429. doi: 10.1099/mic.0.044065-0

Llobet, E., March, C., Giménez, P., and Bengoechea, J. A. (2009). Klebsiella pneumoniae OmpA confers resistance to antimicrobial peptides. *Antimicrobial Agents Chemother.* 53, 298–302. doi: 10.1128/AAC.00657-08

Mandin, P., and Johansson, J. (2020). Feeling the heat at the millennium: Thermosensors playing with fire. *Mol. Microbiol.* 113, 588–592. doi: 10.1111/mmi.14468

Mathers, A. J., Peirano, G., and Pitout, J. D. D. (2015). The role of epidemic resistance plasmids and international high-risk clones in the spread of multidrug-resistant Enterobacteriaceae. *Clin. Microbiol. Rev.* 28, 565–591. doi: 10.1128/CMR.00116-14

McCallum, K. L., and Whitfield, C. (1991). The rcsA gene of Klebsiella pneumoniae O1:K20 is involved in expression of the serotype-specific K (capsular) antigen. *Infect. Immun.* 59, 494–502. doi: 10.1128/iai.59.2.494-502.1991

Ménard, G., Rouillon, A., Cattoir, V., and Donnio, P.-Y. (2021). Galleria mellonella as a suitable model of bacterial infection: past, present and future. *Front. Cell. Infect. Microbiol.* 11. doi: 10.3389/fcimb.2021.782733

Mike, L. A., Starki, A. J., Forsyth, V. S., Vornhagen, J., Smith, S. N., Bachman, M. A., et al. (2021). A systematic analysis of hypermucoviscosity and capsule reveals distinct and overlapping genes that impact Klebsiella pneumoniae fitness. *PloS Pathog.* 17. doi: 10.1371/journal.ppat.1009376

Niu, C., and Gilbert, E. S. (2004). Colorimetric method for identifying plant essential oil components that affect biofilm formation and structure. *Appl. Environ. Microbiol.* 70, 6951–6956. doi: 10.1128/AEM.70.12.6951-6956.2004

Padilla, E., Llobet, E., Doménech-Sánchez, A., Martínez-Martínez, L., Bengoechea, J. A., and Albertí, S. (2010). Klebsiella pneumoniae AcrAB efflux pump contributes to antimicrobial resistance and virulence. *Antimicrobial Agents Chemother.* 54, 177–183. doi: 10.1128/AAC.00715-09

Pan, Y.-J., Fang, H.-C., Yang, H.-C., Lin, T.-L., Hsieh, P.-F., Tsai, F.-C., et al. (2008). Capsular polysaccharide synthesis regions in Klebsiella pneumoniae serotype K57 and a new capsular serotype. *J. Clin. Microbiol.* 46, 2231–2240. doi: 10.1128/JCM.01716-07

Pereira, M. F., Rossi, C. C., da Silva, G. C., Rosa, J. N., and Bazzolli, D. M. S. (2020). Galleria mellonella as an infection model: an in-depth look at why it works and practical considerations for successful application. *Pathog. Dis.* 78. doi: 10.1093/femspd/ftaa056

Russo, T. A., and Marr, C. M. (2019). Hypervirulent klebsiella pneumoniae. *Clin. Microbiol. Rev.* 32. doi: 10.1128/CMR.00001-19

Russo, T. A., Olson, R., Fang, C.-T., Stoesser, N., Miller, M., MacDonald, U., et al. (2018). Identification of Biomarkers for Differentiation of Hypervirulent Klebsiella pneumoniae from Classical K. pneumoniae. *J. Clin. Microbiol.* 56. doi: 10.1128/JCM.00776-18

Schaufler, K., Semmler, T., Pickard, D. J., de Toro, M., de la Cruz, F., Wieler, L. H., et al. (2016). Carriage of Extended-Spectrum Beta-Lactamase-Plasmids Does Not Reduce Fitness but Enhances Virulence in Some Strains of Pandemic E. coli Lineages. *Front. Microbiol.* 7. doi: 10.3389/fmicb.2016.00336

Shankar, C., Vasudevan, K., Jacob, J. J., Baker, S., Isaac, B. J., Neeravi, A. R., et al. (2022). Hybrid plasmids encoding antimicrobial resistance and virulence traits among hypervirulent klebsiella pneumoniae ST2096 in India. *Front. Cell. Infect. Microbiol.* 12. doi: 10.3389/fcimb.2022.875116

Shon, A. S., Bajwa, R. P. S., and Russo, T. A. (2013). Hypervirulent (hypermucoviscous) Klebsiella pneumoniae: a new and dangerous breed. *Virulence* 4, 107–118. doi: 10.4161/viru.22718

Struve, C., Bojer, M., and Krogfelt, K. A. (2008). Characterization of Klebsiella pneumoniae type 1 fimbriae by detection of phase variation during colonization and infection and impact on virulence. *Infect. Immun.* 76, 4055–4065. doi: 10.1128/IAI.00494-08

Xu, C., Shi, W., and Rosen, B. P. (1996). The chromosomal arsR gene of Escherichia coli encodes a trans-acting metalloregulatory protein. *J. Biol. Chem.* 271, 2427–2432. doi: 10.1074/jbc.271.5.2427

Yang, J. C., Lessard, P. A., Sengupta, N., Windsor, S. D., O'brien, X. M., Bramucci, M., et al. (2007). TraA is required for megaplasmid conjugation in Rhodococcus erythropolis AN12. *Plasmid* 57, 55–70. doi: 10.1016/j.plasmid.2006.08.002

Zhang, S., and Meyer, R. (1997). The relaxosome protein MobC promotes conjugal plasmid mobilization by extending DNA strand separation to the nick site at the origin of transfer. *Mol. Microbiol.* 25, 509–516. doi: 10.1046/j.1365-2958.1997.4861849.x